Effects of Temperature and Ocean Acidification on the Extrapallial Fluid pH, Calcification Rate, and Condition Factor of the King Scallop Pecten maximus

Authors: Cameron, Louise P., Reymond, Claire E., Müller-Lundin, Fiona, Westfield, Isaac, Grabowski, Jonathan H., et al.

Source: Journal of Shellfish Research, 38(3) : 763-777

Published By: National Shellfisheries Association

URL: https://doi.org/10.2983/035.038.0327

Journal of Shellfish Research, Vol. 38, No. 3, 763–777, 2019.

EFFECTS OF TEMPERATURE AND OCEAN ACIDIFICATION ON THE EXTRAPALLIAL FLUID pH, CALCIFICATION RATE, AND CONDITION FACTOR OF THE KING SCALLOP *PECTEN MAXIMUS*

LOUISE P. CAMERON,[1,2]* CLAIRE E. REYMOND,[2] FIONA MÜLLER-LUNDIN,[1] ISAAC WESTFIELD,[1] JONATHAN H. GRABOWSKI,[1] HILDEGARD WESTPHAL[2,3] AND JUSTIN B. RIES[1,2]*

[1]*Department of Marine and Environmental Sciences, Northeastern University Marine Science Center, 430 Nahant Road, Nahant, 01908;* [2]*The Leibniz Centre for Tropical Marine Research (ZMT), Fahrenheitstraße 6, Bremen, Germany, 28359;* [3]*University of Bremen, Bibliothekstraße 1, Bremen, Germany, 28359*

ABSTRACT Increasing anthropogenic carbon dioxide is predicted to cause declines in ocean pH and calcium carbonate saturation state over the coming centuries, making it potentially harder for marine calcifiers to build their shells and skeletons. One mechanism of resilience to ocean acidification is an organism's ability to regulate pH and, thus, calcium carbonate saturation state, at its site of calcification. This mechanism has received detailed study in scleractinian corals but is relatively understudied in other taxonomic groups that are vulnerable to ocean acidification, such as bivalves. Here, the results of a 74-day controlled laboratory experiment investigating the impact of ocean acidification on the extrapallial fluid (EPF; the bivalve calcifying fluid) pH, calcification rate, and condition factor of the king scallop *Pecten maximus* at their average spring and summer temperatures (362 ppm/9.0°C, 454 ppm/12.3°C; 860 ppm/9.0°C, 946 ppm/12.3°C; 2,639 ppm/8.9°C, 2,750 ppm/12.1°C) are presented. Scallop EPF pH was lower than seawater pH in all treatments and declined with increasing pCO_2 under the spring temperature (9°C) but was uncorrelated with pCO_2 under the summer temperature (12°C). Furthermore, king scallop calcification rate and EPF pH were inversely correlated at 9°C and uncorrelated at 12°C. This inverse correlation between EPF pH and scallop calcification rate, combined with the observation that scallop EPF pH is consistently lower than seawater pH, suggests that pH regulation is not the sole mechanism by which scallops concentrate carbonate ions for calcification within their EPF. Calcification trends contrasted most other published studies on bivalves, increasing with ocean acidification under spring temperature and exhibiting no response to ocean acidification under summer temperature. Scallop condition factor exhibited no response to ocean acidification under spring temperature but increased with ocean acidification under summer temperature—exactly the opposite of their calcification response to ocean acidification. These results suggest that king scallops are relatively resilient to CO_2-induced ocean acidification, but that their allocation of resources between tissue and shell production in response to this stressor varies seasonally.

KEY WORDS: *Pecten maximus*, ocean acidification, king scallop, extrapallial fluid pH, calcification, condition factor

INTRODUCTION

Since the start of the Industrial Revolution, human activities have caused the partial pressure of atmospheric CO_2 (pCO_2) to increase from 280 ppm to present day levels of *ca.* 410 ppm (Brierley & Kingsford 2009, IPCC 2014). The continued rise in anthropogenic atmospheric CO_2 over the 21st century is predicted to increase average sea surface temperature by *ca.* 0.3°C–1.7°C and to decrease average ocean pH by *ca.* 0.14–0.3 units (IPCC 2014), the latter of which shall be accompanied by a commensurate decline in the calcium carbonate saturation state of seawater (Caldeira & Wickett 2003, Feely et al. 2010). Numerous studies have documented the detrimental effects of ocean acidification on marine organisms, particularly those that build calcium carbonate shells and skeletons. These impacts include reduced calcification rates (e.g., Iglesias-Rodriguez et al. 2008, Ries et al. 2009, Amaral et al. 2012, Andersson & Gledhill 2013, Reymond et al. 2013), shell dissolution (e.g., Ries et al. 2016), altered shell structure (e.g., Welladsen et al. 2010, Gaylord et al. 2011, Horvath et al. 2016), changes in shell mineralogy (e.g., Andersson et al. 2008, Zhuravlev & Wood 2009, Ries 2011b), modified predator–prey dynamics (e.g., Dixson et al. 2010, Ferrari et al. 2011, Kroeker et al. 2014, Dodd et al. 2015), impaired development (e.g., Dupont et al. 2008, Talmage & Gobler 2009, Watson et al. 2009, Brennand et al. 2010), and tissue acidosis (e.g., Pörtner et al. 1998, Michaelidis et al. 2005).

Bivalves are particularly vulnerable to the impacts of ocean acidification because they are primarily sessile and, thus, generally unable to migrate to higher pH waters, rendering them susceptible to whatever conditions exist at a given location (Michaelidis et al. 2005). Ocean acidification also commonly causes tissue acidosis and hypercapnia in bivalves because they are osmoconformers (i.e., maintain their internal environment in osmotic equilibrium with their external environment; Pörtner 2008). Furthermore, bivalves rely almost exclusively on their shell for protection from predators—meaning that a loss of shell strength due to ocean acidification translates directly to increased mortality. Although bivalves are reportedly more sensitive to ocean acidification than most other groups of calcifying marine organisms (e.g., Melzner et al. 2011, Amaral et al. 2012, Gazeau et al. 2013, Hiebenthal et al. 2013, Kroeker et al. 2013, Waldbusser et al. 2015), this class of molluscs still exhibits a high degree of interspecific variability in their vulnerability to ocean acidification (Ries et al. 2009). Impacts vary widely among species and life stages, with some species exhibiting high sensitivity to ocean acidification (e.g., the eastern oyster *Crassostrea virginica*, Ries et al. 2009, Talmage & Gobler 2011, Waldbusser et al. 2011) and others exhibiting resilience to

*Corresponding authors. E-mail: cameron.lo@husky.neu.edu or j.ries@northeastern.edu
DOI: 10.2983/035.038.0327

ocean acidification (e.g., the blue mussel *Mytilus edulis*; Ries et al. 2009, Hiebenthal et al. 2013, Mackenzie et al. 2014). Larvae are also generally reported to be more vulnerable to ocean acidification than their adult counterparts (Talmage & Gobler 2011, Waldbusser et al. 2014, Waldbusser et al. 2015, Frieder et al. 2017). An improved understanding of the factors influencing the responses of bivalves to ocean acidification should inform predictions of their relative vulnerability or resilience to future ocean acidification.

The high commercial value of marine bivalves makes their sensitivity to ocean acidification as much a socioeconomic as an ecological concern. Yet, few studies have addressed the impacts of ocean acidification on pectinids (scallops). A prior study on the king scallop *Pecten maximus* (Sanders et al. 2013) found tissue growth within this species to be fairly resilient to ocean acidification, but calcification rates of the juvenile and adult bay scallop *Argopecten irradians* decreased under conditions of elevated pCO_2 (Ries et al. 2009, White et al. 2013). A better understanding of the impacts of ocean acidification on scallop tissue and shell production is needed to determine how future anthropogenic oceanic change will affect the valuable fisheries supported by scallops.

Seasonal fluctuations in seawater temperature cause substantial changes in the calcium carbonate saturation state of seawater, especially in higher latitude oceans (Orr et al. 2005). In addition, energetic requirements of marine bivalves fluctuate with seasonal spawning cycles, where shell and tissue growth are asynchronous (Hilbish 1986). A trade-off in energy allocated between reproduction and calcification has been identified in other calcifying taxa, such as tropical scleractinian corals (Cabral-Tena et al. 2013), and this is also likely to exist in bivalves. Ocean acidification may, therefore, elicit different responses in bivalves at different times of the year because of season-specific energetic requirements for reproduction and/or shell growth. Although the effects of ocean acidification on bivalves over seasonal temperature cycles have not been studied, the combined effects of ocean acidification and warming have been investigated. Warming decreased bivalve survivorship (Byrne 2011), growth (Beukema et al. 2009), and larval recruitment (Beukema & Dekker 2005, Beukema et al. 2009), whereas investigations of the combined effects of acidification and warming have yielded mixed results. Although some studies have found that temperature and acidification have additive, negative effects on marine bivalves (Talmage & Gobler 2009, Talmage & Gobler 2011), others have shown that acidification partially mitigates the negative impacts of warming (Ivanina et al. 2013), and *vice versa* (Parker et al. 2010).

Bivalve shells are biomechanically sophisticated, multilayered structures built from the calcium carbonate minerals calcite and/or aragonite. The formation of bivalve shells occurs within a semienclosed fluid between the mantle and the inner shell layer, known as the extrapallial fluid (EPF; Crenshaw 1972). This fluid acts as a reservoir and assembly point for shell constituents (Wheeler & Sikes 1984) and contains numerous polypeptides whose functions include the initiation and inhibition of shell growth (Weiner & Traub 1984, Wilbur & Bernhardt 1984), control of crystal morphology and polymorph mineralogy (Wheeler & Sikes 1984), and the binding of calcium ions (de Jong et al. 1976). Although much about bivalve mineralization is still unknown, the presence of a complex array of macromolecules within the EPF strongly suggests that the EPF plays an important role in the initiation and control of bivalve calcification. The inorganic composition of the EPF reinforces this, as calcium and dissolved inorganic carbon (DIC) are concentrated here relative to both bivalve hemolymph and external seawater (Crenshaw 1972). The chemistry at the site of calcification in marine organisms has been proposed to play a key role in dictating their specific responses to ocean acidification (Ries et al. 2009). Studies show that other taxa elevate pH of their calcifying fluid relative to seawater pH (Al-Horani et al. 2003, Ries 2011a, Trotter et al. 2011, Venn et al. 2011, Mcculloch et al. 2012a, 2012b, Holcomb et al. 2014, Hohn & Merico 2015, Wall et al. 2015, Cai et al. 2016, Sutton et al. 2018), potentially by using enzymes such as Ca^{2+}/H^+-ATPase to exchange hydrogen ions in the calcifying fluid for calcium ions in the surrounding seawater (Cohen & McConnaughey 2003). This exchange increases calcification site pH and shifts the carbonate system equilibria in the fluid toward increased concentrations of CO_3^{2-} ($[CO_3^{2-}]$) and Ca^{2+} ($[Ca^{2+}]$), thereby increasing calcium carbonate saturation state at the site of calcification.

Interestingly, bivalve EPF pH is typically *ca*. 0.5–0.6 units lower than seawater pH, with shell calcification proceeding even when EPF pH is as low as 7.0–7.2 (Crenshaw 1972). The observation that the concentration of DIC within the EPF of mussels, clams, and oysters is approximately double that of seawater (Crenshaw 1972) suggests that the combination of elevated DIC and elevated pH (relative to equilibrium pH associated with the elevated DIC) in the EPF may elevate its calcium carbonate saturation state, thereby supporting precipitation of calcium carbonate—as also recently proposed for scleractinian corals (e.g., McCulloch et al. 2017).

Despite the established importance of the EPF in bivalve biomineralization, its role in dictating the response of bivalves to ocean acidification has been little explored. The few studies investigating the role of the EPF in responses to ocean acidification have been largely focused on the larval stage of bivalve development. The apparent sensitivity of blue mussel *Mytilus edulis* larvae to ocean acidification has been linked to corresponding decreases in EPF pH and $[CO_3^{2-}]$ (and thus $CaCO_3$ saturation state of the EPF) measured with microelectrodes (Ramesh et al. 2017). Likewise, the sensitivity of oyster larvae *Magallana gigas* (formerly known as *Crassostrea gigas*) to ocean acidification has been attributed to their weaker ability to isolate and chemically control their EPF compared with later life stages (Waldbusser et al. 2013), which may arise from physiological and energetic differences between adult and larval bivalves, as well as from differences in the polymorph mineralogy and function of the shells formed by adult versus larval bivalves (Addadi et al. 2006, Gazeau et al. 2013).

To investigate the role that EPF pH regulation plays in the response of the economically important king scallop *Pecten maximus* to CO_2-induced ocean acidification, this species was cultured in a fully crossed pCO_2 and temperature experiment for a 74-day period. Calcification rates were estimated from the change in scallop buoyant weight between the beginning and the end of the experiment, condition factor was assessed at the end of the experiment, and EPF pH was measured with proton-sensitive liquid ion-exchanger (LIX) microelectrodes during the final week of the experiment. The previously observed resilience of king scallops to ocean acidification (Sanders et al. 2013) suggests that this species should be able to maintain relatively constant calcification rates across pCO_2 treatments. It was hypothesized that this relative resilience would be linked to strong regulation of EPF pH, requiring additional energetic input under elevated pCO_2, potentially leading to a decline in Fulton's condition factor (a proxy for physiological fitness). It was also hypothesized that temperature

would affect this response, as energetic investment into different physiological processes, such as reproduction versus calcification, varies seasonally and may, therefore, depend on the thermal environment of the organism.

MATERIALS AND METHODS

Experimental Design

King scallops *Pecten maximus* with a shell height of 84.1–103.0 mm (mean = 94.4 mm) were collected by SCUBA from Sea Box SM16, Sound of Mull (GPS 56.6109 N, 6.3905 W), Scotland, in March 2016. Scallops were then transported on ice to the Leibniz Center for Tropical Marine Research (ZMT, Bremen, Germany), where they were acclimated to laboratory conditions (temperature ± SE = 9.0 ± 0.0°C, salinity ± SE = 34.6 ± 0.0 ppt, pH ± SE = 8.1 ± 0.0) for 14 days and subsequently reared for 74 days (April–June 2016) under two temperatures crossed with three pCO_2 regimes, corresponding to present day conditions (temperature ± SE/pCO_2 ± SE = 9.0 ± 0.0°C/362 ± 6 ppm; 12.3 ± 0.0°C/454 ± 12 ppm), the IPCC RCP 6.0 year 2100 scenario (IPCC 2014, temperature ± SE/pCO_2 ± SE = 9.0 ± 0.0°C/860 ± 31 ppm; 12.3 ± 0.0°C/946 ± 42 ppm), and a year 2500 scenario (T ± SE/pCO_2 ± SE = 8.9 ± 0.0°C/2,639 ± 78 ppm; 12.1 ± 0.1°C/2,750 ± 110 ppm). Temperature treatments represent average spring (9°C) and summer (12°C) seawater temperatures at Oban, Scotland (Curry 1982), which is near the scallop collection site. Each scallop was fed 2.5 mL of a microalgae-based commercial shellfish food (Shellfish Diet 1800) diluted in 7.5 mL seawater. Scallops were fed once per day, at which time, the seawater filtration systems were bypassed for 30 min to allow scallops to filter the suspended algae. Five replicate tanks were used per treatment, with each replicate tank housing one scallop. Calcification rates were estimated from the percent change in buoyant weight of the specimens between the beginning and end of the experiment. Microelectrode measurements of scallop EPF pH were obtained over a 7-day period at the end of the experiment.

Measurement and Control of Seawater Carbonate Chemistry

Compressed CO_2-free air and compressed CO_2 were blended using solenoid-valve mass flow controllers to produce gas mixtures formulated at the target pCO_2 conditions. These gas mixtures were then bubbled into six 284-L flow-through experimental seawater systems, each consisting of two seawater reservoirs and five 2-L replicate aquaria. Temperature was controlled with 1650-W aquarium chillers (Aqua Medic Titan 2000). Experimental treatment water was refreshed with natural seawater (obtained from Spitzbergen, Norway, and stored at ZMT) at a rate of 0.6 L/h. This rate was sufficiently slow to allow near-equilibrium to be reached between the mixed gases and the experimental seawaters, yet fast enough to prevent material alteration of the dissolved constituents of the experimental seawaters through calcification or waste excretion. Temperature, pH, and salinity of all replicate tanks (n = 5) were measured three times per week using a combination probe kit (WTW Multi 3430 Set K). Before each use, the pH electrode was calibrated with pH 4.00 and 7.00 NBS buffers traceable to NIST standard reference material at both treatment temperatures, and the conductivity (salinity) probe was calibrated with certified seawater reference material of 33.347 salinity (Dickson CRM batch #154) at both treatment temperatures. Seawater samples for the analysis of DIC and total alkalinity (TA) were collected weekly from each replicate tank, with TA samples stored in 50-mL polypropylene centrifuge tubes and DIC samples stored in 25-mL borosilicate glass vials sealed with rubber septae. After collection, DIC and TA samples were poisoned with 10 and 20 µm, respectively, of saturated mercuric chloride solution and refrigerated until analysis. Total alkalinity was measured by open-cell potentiometric Gran titration (accuracy = ±20 µmol/kg). Dissolved inorganic carbon was measured with a Shimadzu DIC analyzer (accuracy = ±10 µmol/kg). Seawater pCO_2, pH (seawater scale), carbonate ion concentration ($[CO_3^{2-}]$), bicarbonate ion concentration ($[HCO_3^-]$), aqueous CO_2, and calcite saturation state (Ω_c) were calculated from measured TA and DIC with the program CO_2SYS (Lewis & Wallace 1998), using Roy et al. (1993) values for the K_1 and K_2 carbonic acid constants, the Mucci (1983) value for the stoichiometric calcite solubility product, and an atmospheric pressure of 1.015 atm (Table 1).

Measurement of Calcification Rates

Calcification rates were calculated from the change in buoyant weight of the scallop specimens (n = 30) between the beginning and end of the experiment. Buoyant weights were obtained by placing scallops on a platform hung from a bottom loading scale (Mettler Toledo, precision = 0.01 g), with the platform suspended at a fixed depth in seawater of constant temperature and salinity. Scallops were weighed three times to obtain a mean weight. Scallops were reweighed if repeat measurements varied by more than 0.05 g. A standard of known weight was measured every five samples to ensure that the scale was functioning properly (i.e., no instrumental drift). The relationship between the dry and buoyant weights of the scallop shells was empirically defined by plotting dry weight of the shells (determined at the completion of the experiment) against their corresponding buoyant weights at that time (Fig. 1; method previously established for bivalves by Ries et al. 2009). This relationship can be defined for the king scallops from this experiment with the following algorithm:

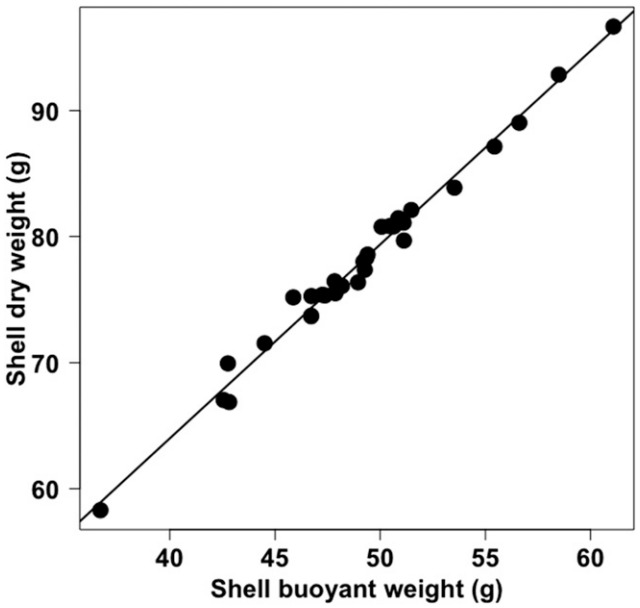

Figure 1. Linear relationship between measured buoyant weights and dry weights of the king scallop shells at completion of experiment (y = 1.537x + 2.500, P < 0.001, R^2 = 0.986, SE = 0.034).

TABLE 1.

Average measured seawater parameters: salinity, temperature, pH on NBS scale (pH_{NBS}), total alkalinity (TA), and DIC.

Measured parameters		Control pCO_2		Moderate pCO_2		High pCO_2	
		9°C	12°C	9°C	12°C	9°C	12°C
Salinity	(psu)	34.93	35.25	34.99	35.59	35.08	35.56
	SE	0.02	0.03	0.02	0.03	0.02	0.03
	Range	34.14–35.25	34.55–35.85	34.05–35.55	34.75–36.15	34.55–36.65	34.65–36.25
	n	128	115	140	140	118	125
Temperature	(°C)	9.0	12.3	9.0	12.3	8.9	12.1
	SE	0.0	0.0	0.0	0.0	0.0	0.0
	Range	8.3–10.8	11.6–12.8	8.4–10.2	11.2–13.0	8.2–10.2	11.4–13.0
	n	128	114	140	138	118	123
pH_{NBS}		8.05	8.09	7.82	7.85	7.41	7.42
	SE	0.01	0.01	0.01	0.01	0.01	0.01
	Range	7.52–8.26	7.78–8.33	7.46–7.96	7.43–8.04	7.11–7.67	7.09–7.60
	n	124	110	135	135	115	119
TA	(μM)	3,271	3,380	3,135	3,133	3,283	3,183
	SE	98	120	64	71	55	76
	Range	2,354–3,851	2,610–4,222	2,601–3,593	2,595–3,743	2,755–3,583	2,583–3,607
	n	31	27	35	35	26	26
DIC	(μM)	3,076	3,147	3,050	3,044	3,322	3,267
	SE	87	102	62	66	63	72
	Range	2,189–3,603	2,359–3,748	2,524–3,470	2,500–3,564	2,826–3,683	2,707–3,639
	n	31	27	35	35	26	26
		Calculated parameters					
pCO_2	(ppm)	362	454	860	946	2,639	2,750
	SE	6	12	31	44	78	110
	Range	300–408	339–523	620–1,256	600–1,702	1,842–3,371	1,880–3,793
	n	31	27	35	35	26	26
pH_{sw}		8.31	8.26	7.95	7.92	7.56	7.52
	SE	0.02	0.00	0.03	0.03	0.03	0.02
	Range	8.16–8.46	8.05–8.34	7.41–8.12	7.38–8.10	7.12–7.65	7.19–7.71
	n	31	27	35	35	26	26
$[CO_3^{2-}]$	(μM)	289	287	140	151	60	63
	SE	17	15	6	6	3	3
	Range	146–448	185–406	64–176	68–207	26–79	46–80
	n	31	27	32	35	26	25

continued on next page

TABLE 1.
continued

Measured parameters		Control pCO_2		Moderate pCO_2		High pCO_2	
		9°C	12°C	9°C	12°C	9°C	12°C
$[HCO_3^-]$	(μM)	2,746	2,809	872	2,842	3,175	3,137
	SE	71	89	58	61	61	69
	Range	2,025–3,141	2,132–3,359	2,396–3,335	2,335–3,355	2,667–3,494	2,570–3,452
	n	31	27	35	35	26	26
$[CO_2]_{(sw)}$	(μM)	18	20	40	39	113	112
	SE	1	1	2	2	5	5
	Range	14–23	14–30	28–61	25–68	81–189	64–155
	n	31	27	35	35	26	25
Ω_c		6.9	6.8	3.3	3.6	1.4	1.5
	SE	0.4	0.3	0.2	0.1	0.1	0.1
	Range	3.5–10.7	4.4–9.7	1.6–4.6	1.6–4.9	0.8–1.9	1.0–1.9
	n	31	27	35	35	26	26

Average calculated seawater parameters: partial pressure of carbon dioxide (pCO_2) of the mixed gases in equilibrium with the experimental seawaters, pH on the seawater scale (pH_{SW}), carbonate ion concentration ($[CO_3^{2-}]$), bicarbonate ion concentration ($[HCO_3^-]$), dissolved CO_2 ($[CO_2]_{(SW)}$), and calcite saturation state (Ω_C). *n*, number of observations.

$$\text{Dry weight (g)} = 1.537 \times \text{buoyant weight} + 2.500,$$

where the precision of the scallop buoyant weight as an estimator of their dry weight is equivalent to the SE of the regression (0.034 g). This relationship was then used to convert measured buoyant weights to dry weights, with net calcification rates expressed as the %-change in dry weight of the shell to control for the allometric relationship between scallop shell size (mass) and calcification rate.

Microelectrode Measurements of Scallop EPF pH

Scallop EPF pH was measured during the final week of the experiment, shortly after obtaining the final buoyant weight of each specimen. A 3-mm hole was drilled into the central rib of the right valve of each scallop at a distance from the umbo of approximately 1/3 the shell height. The drilling site was flushed with seawater during drilling to reduce friction and heating. Immediately after drilling, a 1-mm-diameter plastic pipette tip was cut to a length of 5 mm and epoxied into the drilled hole to serve as a port for inserting the microelectrode into the EPF. The open end of the port was sealed with paraffin film to prevent seawater from entering the EPF. Scallops were then returned to their tanks and reacclimated to their treatment conditions for 2 days before EPF pH measurement.

The pH microelectrodes were produced at the Max Planck Institute of Marine Microbiology (MPIMM) using the technique described by de Beer et al. (1997). Briefly, green soda lime glass tubes (Schott model 8516) were exposed to a heated coil and pulled into microcapillary tubes with a target tip diameter of *ca.* 10 μm. The microcapillary tubes were then silanized to obtain a hydrophobic surface to which the LIX membrane would adhere. Microelectrodes were filled with *ca.* 300 μm of degassed, filtered (0.2-μm Millipore membrane) electrolyte (300 mM KCl and 50 mM sodium phosphate adjusted to pH 7.0) using a plastic syringe with a 0.1-mm tip. The capillaries were then backfilled with LIX containing a polyvinyl acetate epoxy to prevent leakage of electrolyte. This was performed by dipping the capillary tips in the LIX and applying suction until 100–200 μm of the polyvinyl acetate–containing LIX was drawn into the capillary tip. Microcapillary tubes were encased in a Pasteur pipette for shielding, with the pulled tip of the microcapillary tube protruding *ca.* 2 cm beyond this casing. The casing was filled with a 0.3 M KCl solution and connected to the reference electrode with an Ag/AgCl wire to minimize electrical noise in the system. Microelectrodes with a tip diameter of between 8 and 20 μm were filled with LIX-positive and LIX-negative pH membranes. Microelectrodes were left for 24 h after construction to allow stabilization of the LIX membranes.

All microelectrode equipment (millivolt meter, National Instruments DAQ Pad 6020E, laptop, cables, micromanipulator, VT80 Micos motor arm, laboratory stands, Zeiss Stemi SV6 binocular microscope) was set up adjacent to the experimental tanks to minimize the stress of transporting the scallops. Two reservoirs of seawater, sourced from the corresponding experimental treatment tanks, were established next to the microelectrode system. These reservoirs were bubbled with the corresponding treatment gases and maintained at the treatment temperature using aquarium chillers. The seawater was circulated between the two reservoirs through two 5.4-L flow-through chambers (30 × 12 × 15 cm). All pH microelectrode measurements were performed within these smaller flow-through chambers.

The pH microelectrodes were calibrated before and after EPF measurements using pH 7.00 and 9.00 NBS buffers (to obtain the slope of the pH-mV calibration) traceable to NIST standard reference material, and a Dickson seawater CRM ($pH_{SW} = 7.817$; to obtain the *y*-intercept of the pH-mV calibration). All buffers and standards were maintained at the two treatment temperatures. The microsensor was vertically positioned with a computer-controlled motorized micromanipulator with a precision of 1 μm.

Extrapallial fluid pH was measured in three scallops per experimental treatment. Scallop shells were maintained in a slightly opened position (*ca.* 5 mm) during measurement of EPF pH by inserting a 5-mm-thick strip of plastic between their shells. This ensured that EPF pH was measured while the scallops were in typical resting position (i.e., feeding with shells open and with scallop tissue in direct contact with circulating seawater), rather than the closed position that they maintain for only short intervals when stressed or threatened—which could cause EPF chemistry to deviate from typical conditions because of build-up of respired CO_2 and other waste products. The pH microelectrode was lowered through the paraffin film, through the microsensor port, and ultimately into the EPF of the scallop. Once the voltage signal stabilized (*ca.* 5 min), a pH profile of the EPF, port, and seawater adjacent to the scallop was generated by moving the microelectrode out of the port in 50-μm steps (Fig. 2).

Measurement of Scallop Condition Factor (Fulton's K)

All tissue was extracted from the scallop shells at the end of the experiment, blotted dry, and weighed. Shell height was measured to the nearest millimeter with calipers. Scallop condition factor (Fulton's K) was then calculated as follows:

$$\text{Condition Factor} = TW_{WET}/SH^3,$$

where "TW_{WET}" is the wet weight of the whole tissue and "SH" is the shell height (distance from umbo to ventral margin). Shell height was cubed according to standard allometric scaling practice (Lucas & Beninger 1985) so that measurements of both tissue and shell varied on a cubic scale.

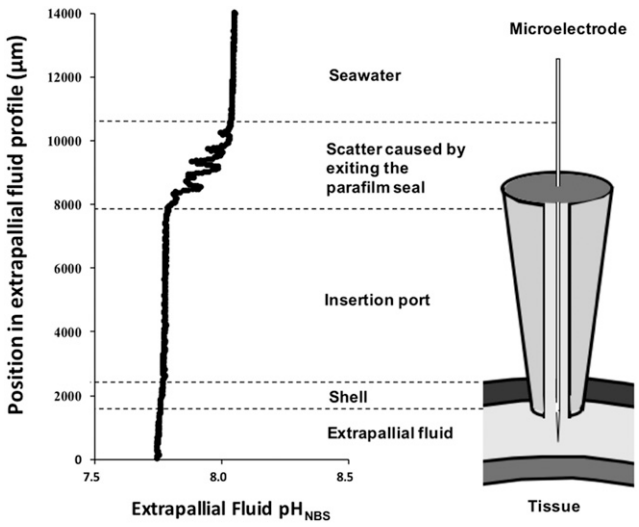

Figure 2. Diagram illustrating insertion of the proton-sensitive LIX microelectrode through the shell port into the EPF of a king scallop (right) and the corresponding pH_{NBS} profile (left) obtained by moving the microelectrode upward from the mantle, through the EPF, shell port, and ultimately into the surrounding seawater.

Data Processing and Statistical Analysis

The voltage output of the microelectrode measurements was converted to pH using the calibration regressions described previously. Fluid pH profiles were then generated by plotting measured pH against distance of the microelectrode from its starting position. The pH profiles, annotated with relative location data recorded during the microelectrode measurements, were then divided into three spatial zones: EPF, shell port, and external seawater (Fig. 1). Mean pH was calculated for each zone.

All statistical analyses were performed using the program R Studio (version 0.99.903). General linear models (GLM) were used to test how calcification rate, EPF pH, and condition factor respond to pCO_2, temperature, and the interaction between these predictors. Various models were run in the order of decreasing complexity, and Akaike Information Criterion (AIC) was used to identify the optimal model (Tables A1–A4). Models were run with and without EPF pH as a predictor of calcification rate because this variable was measured for only a subset of individuals. Owing to the low sample size within treatments ($n = 5$ for models excluding EPF pH, $n = 3$ for models including EPF pH), an alpha of 0.1 was used to reduce the potential for type 2 errors (Gotelli & Ellison 2013). When predictor variables exhibited an obvious difference in trend under the two temperature regimes, or when the interaction term *P* value was less than 0.2, the models were run for each temperature treatment separately to permit interpretation of the main effects at each level of the interaction (Carey 2013). To investigate the seasonal impacts of ocean acidification, a paired *t*-test was used to test whether the slopes of each response to ocean acidification, and their direction, were different under the two seasonal temperature scenarios.

The assumptions of each GLM were tested by generating diagnostic plots to examine homoscedasticity and normality of residuals. A plot of residuals versus fitted values and a scale location plot were used to examine homoscedasticity, and a quantile–quantile plot was used to examine normality. Normality of residuals was further tested for each model with a Shapiro–Wilk test, and all models met this assumption.

RESULTS

Calcification Rate

Calcification rate was best predicted (pursuant to AIC) by a model that included the effects of pCO_2, temperature, and their interaction (Table A1). Because the response of calcification rate to pCO_2 was markedly different under the two temperature regimes (Fig. 3A), consistent with the low *P* value of the temperature–pCO_2 interaction term ($P < 0.2$, see Methods), the effects of pCO_2 on calcification rate were tested separately at 9°C and 12°C (Table 2). At 9°C, calcification rate (Fig. 3A) increased significantly with increasing pCO_2 (Table 2, GLM, $P = 0.097$), whereas calcification rate did not significantly vary with pCO_2 at 12°C (Table 2, GLM, $P = 0.377$). The slope of the scallop calcification response to increasing pCO_2 was significantly more positive at 9°C than at 12°C (Table 3, paired *t*-test, $P = 0.051$, $t = 1.7$, df = 26).

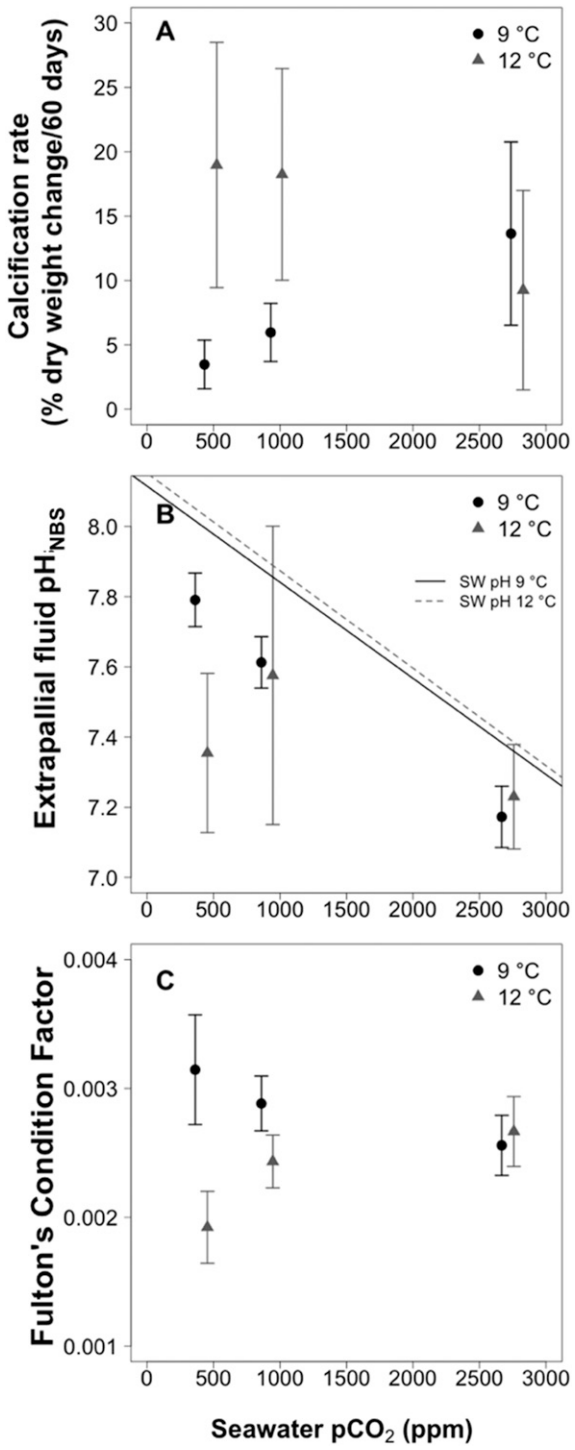

Figure 3. Treatment pCO_2 versus scallop calcification rate (A), EPF pH_{NBS} (B), and condition factor (C) of the king scallop *Pecten maximus* at 9°C (circle) and 12°C (triangle). Vertical error bars represent 1 SE of each response variable and horizontal error bars represent 1 SE of the calculated pCO_2 across replicate tanks. Trend lines in panel B represent measured seawater pH at 9°C (solid black line) and 12°C (dashed gray line). (A) Increasing pCO_2 significantly increased scallop calcification rate at 9°C ($P = 0.097$), but did not impact calcification rate at 12°C ($P = 0.377$). (B) Increasing pCO_2 significantly decreased EPF pH at 9°C ($P = 0.001$) but did not impact EPF pH at 12°C ($P = 0.577$). (C) Increasing pCO_2 significantly increased condition factor at 12°C ($P = 0.089$) but did not impact condition factor at 9°C ($P = 0.210$).

EPF pH

Extrapallial fluid pH (Fig. 3B) was best predicted (pursuant to AIC) by pCO_2 alone (Table A2). This analysis showed that EPF pH and pCO_2 were negatively correlated (Table 2, GLM, $P = 0.048$). Because the response of EPF pH to pCO_2 was markedly different under the two temperature regimes (Fig. 3B), the effect of pCO_2 on EPF pH was also tested separately at each temperature. EPF pH was negatively correlated with pCO_2 at 9°C (Table 2, GLM, $P = 0.001$) but showed no correlation with pCO_2 at 12°C (GLM, $P = 0.577$). EPF pH variance was also substantially higher at 12°C than at 9°C (9°C, SE = 0.00005; 12°C, SE = 0.00016). The slope of the EPF pH response to increasing pCO_2 was significantly more positive at 12°C than at 9°C (Table 3, paired *t*-test, $P = 0.092$, $t = -1.37$, df = 26)—opposite of the calcification responses of scallops to pCO_2 at the two temperatures.

The correlation between EPF pH and calcification rate was also explored (Figure 4, Table A3). In this model, increasing EPF pH and decreasing pCO_2 were significantly correlated with decreasing calcification rate at 9°C (Table 2, GLM, $P = 0.033$). At 12°C, calcification rate was best predicted by a model that included the interaction between EPF pH and pCO_2; however, neither term, nor their interaction, was significantly correlated with calcification rate (GLM, pCO_2: $P = 0.187$; EPF pH: $P = 0.397$; interaction: $P = 0.190$).

Scallop Condition Factor

A GLM that included the effects of pCO_2, temperature, and their interactive effects best predicted condition factor (Fig. 3C, Table A4). The effect of pCO_2 on EPF pH was also tested separately at each temperature because the response of condition factor to pCO_2 was markedly different under the two temperature regimes (Fig. 3C). At 9°C, condition factor was not significantly impacted by increasing pCO_2 (GLM; $P = 0.210$), whereas at 12°C, condition factor significantly increased with increasing pCO_2 (GLM, $P = 0.089$). The slope of the condition factor response to increasing pCO_2 was significantly more positive at 12°C than at 9°C (Table 3, paired *t*-test, $P = 0.016$, $t = -2.28$, df = 26)—similar to the EPF pH responses to pCO_2 at the two temperatures. Notably, condition factor decreased significantly with increasing temperature (GLM, $P = 0.036$).

DISCUSSION

Impact of Ocean Acidification on King Scallop Shell Production

King scallop calcification exhibited relative resilience to the prescribed seawater acidification, with calcification rates remaining constant with increasing pCO_2 under the summer temperature condition and increasing with pCO_2 under the spring temperature condition (Fig. 3). These findings contrast most prior studies that report strong declines in bivalve calcification under future ocean acidification scenarios (e.g., Michaelidis et al. 2005, Melzner et al. 2011, Amaral et al. 2012, Gazeau et al. 2013, Waldbusser et al. 2014), although those investigating the combined stressors of CO_2 and temperature found a weaker response to increasing pCO_2 under elevated temperatures (Waldbusser et al. 2011, Kroeker et al. 2013). Whereas many bivalve species exhibit linear declines in

TABLE 2.

Summary of AIC-selected models for subsequent analysis, along with their corresponding statistical parameters.

Response variable	Model	Temperature	AIC	Predictor variable	SE	*t*-value	*P*-value
Calcification rate	pCO_2	9°C	114.010	pCO_2	0.002	1.787	0.097*
Calcification rate	pCO_2	12°C	133.710	pCO_2	0.005	–0.914	0.377
EPF pH	pCO_2	Both	17.136	pCO_2	<0.001	–2.139	0.048**
	pCO_2	9°C	–5.883	pCO_2	<0.001	–5.368	0.001****
	pCO_2	12°C	16.16	pCO_2	0.002	–0.584	0.577
Condition factor	pCO_2 × temperature	Both	–354.450	pCO_2	<0.001	–2.146	0.041**
				Temperature	<0.001	–3.143	0.004***
				pCO_2 × temperature	<0.001	2.196	0.037**
Condition factor	pCO_2	9°C	–173.120	pCO_2	<0.001	–1.320	0.210
Condition factor	pCO_2	12°C	–177.670	pCO_2	<0.001	1.833	0.089*
Condition factor	Temperature	Both	–351.31	Temperature	<0.001	–2.201	0.036**
Calcification rate (including EPF)	pCO_2 + EPF pH	9°C	57.111	pCO_2	0.004	–2.424	0.052*
				EPF pH	12.093	–2.754	0.033**
Calcification rate (including EPF)	pCO_2 × EPF pH	12°C	20.388	pCO_2	0.137	1.526	0.187
				EPF pH	21.310	0.926	0.397
				pCO_2 × EPF pH	0.019	–1.514	0.190

* Significance at $\alpha = 0.10$.
** Significance at $\alpha = 0.05$.
*** Significance at $\alpha = 0.01$.
**** Significance at $\alpha = 0.001$.

calcification rate in response to declining saturation state at values greater than 1 (Ries et al. 2009, Gazeau et al. 2010, Barton et al. 2012), others only exhibit a decline in calcification rate when the calcium carbonate saturation state of seawater falls below 1 (i.e., undersaturated conditions favoring shell dissolution; Ries et al. 2009, Waldbusser et al. 2014, Waldbusser et al. 2015). It is, therefore, possible that the lack of negative calcification response to ocean acidification in the present study may arise from the calcite saturation states of all experimental treatments remaining above 1 (i.e., supersaturated).

Few studies have addressed the impacts of ocean acidification on pectinids (Ries et al. 2009, Talmage & Gobler 2009, Andersen et al. 2013, Sanders et al. 2013, Schalkhausser et al. 2013, White et al. 2013). Two prior studies found that the growth of scallop larvae decreased under acidified conditions (Talmage & Gobler 2009, Andersen et al. 2013), contrasting the results of the present study. Differences between larval and adult scallop responses to ocean acidification should not be surprising given their differences in physiology, energy reserves, ability to isolate their EPF, shell polymorph mineralogy, shell function, and calcification mechanisms, as well as inherent allometric differences, such as shell surface area-to-volume ratio (Pörtner & Farrell 2008). A prior study on the adult bay scallop *Argopecten irradians* revealed that their calcification rates declined linearly with CO_2-induced ocean acidification (Ries et al. 2009). These different outcomes are further evidence of the wide range of responses to ocean acidification exhibited by different taxa, even within a single family (Pectinidae), and highlight the need for further comparative research into the causes of the resilience or vulnerability of marine calcifiers to this critical aspect of global oceanic change.

TABLE 3.

Summary of *t*-tests investigating differences in the response of king scallop *Pecten maximus* calcification rate, EPF pH, and condition factor to ocean acidification under spring (9°C) vs. summer (12°C) temperature conditions.

Comparison of 9°C and 12°C slopes				
Response variable	**Estimated slope difference**	***t*-value**	**df**	***P*-value**
Calcification rate	0.00879	1.70	26	0.051*
EPF pH	–0.000166	–1.37	26	0.092*
Condition factor	-5×10^{-7}	–2.28	26	0.016**

T-tests evaluated whether slopes generated from the GLMs for each of the measured response variables were significantly different under the two temperature regimes. Estimated slope difference is GLM-generated slope of measured response variable at 9°C minus slope at 12°C. df, degrees of freedom.
* Significance at $\alpha = 0.10$.
** Significance at $\alpha = 0.05$.

Impact of Ocean Acidification and Temperature on King Scallop Condition Factor

Condition factor is commonly used to assess the quality and profitability of commercial fish and shellfish and also to assess the general physiological performance and stress level of an organism (Lucas & Beninger 1985). In the present study, condition factor of the king scallops varied significantly with pCO_2, temperature, and the interaction between seawater pCO_2 and temperature. Specifically, condition factor was not significantly correlated with pCO_2 at 9°C, was significantly positively correlated with pCO_2 at 12°C, and was significantly negatively correlated with increasing temperature—collectively suggesting that king scallop condition factor is relatively resilient to ocean acidification, but vulnerable to warming.

When organisms are stressed, more of their energy budget is diverted toward basal physiological processes, such as maintenance and repair of tissue (Pörtner 2002), which diverts energy from reproduction, production of new tissue, and build-up of lipid reserves and polysaccharides—thereby decreasing their condition factor. Ocean acidification and warming appear to have complex effects on the condition factor of marine bivalves. Thermal stress has been shown to negatively impact condition factor and energetic reserves in a number of bivalve species (Hiebenthal et al. 2013, Ivanina et al. 2013), whereas the impact of ocean acidification on bivalve condition factor appears more nuanced. Although increased pCO_2 can negatively impact the condition factor of some species (e.g., the eastern oyster *Crassostrea virginica*, Beniash et al. 2010, Dickinson et al. 2012), other species have exhibited no change in condition factor in response to elevated pCO_2 (e.g., the blue mussel *Mytilus edulis*, Thomsen & Melzner 2010). Other studies, including the present one on king scallops, have observed an improvement in condition factor in response to increasing pCO_2 (Beniash et al. 2010, Fernández-Reiriz et al. 2011) and mitigation of the impacts of thermal stress under elevated pCO_2, and *vice versa* (Hiebenthal et al. 2013). Given the ecological and economic importance of bivalve species, further investigation of how temperature and ocean acidification interact to influence their condition factor is needed to predict how bivalves will respond to future global oceanic change.

King Scallop Response to Ocean Acidification Varies with Seasonal Temperature

The combined effects of ocean acidification and temperature (across the seasonal range of a species) on bivalves have received little previous study. Notably, the present study showed that all measured performance parameters (EPF pH, condition factor, and calcification rate) exhibited significantly different responses to ocean acidification under the two temperature regimes (Fig. 3, Table 3). Furthermore, calcification rate and condition factor showed opposite responses to ocean acidification under each temperature regime, with calcification rate exhibiting a more positive response to pCO_2 than condition factor at 9°C, and condition factor exhibiting a more positive response to pCO_2 than calcification rate at 12°C (Fig. 5). This opposition of the calcification rate and condition factor responses to ocean acidification at each of the two temperatures (in favor of calcification at 9°C and in favor of condition factor at 12°C) suggests that king scallops exposed to ocean acidification divert excess energy toward tissue production under summer temperatures (12°C) and toward shell production under spring temperatures (9°C).

Although the cause of this apparent diversion of energy from shell to tissue production (with increasing pCO_2) between spring and summer temperatures cannot be unequivocally deduced from the data at hand, it is possible that it reflects seasonal differences in the physiological demands of king scallops. The diversion of energy toward shell production with increasing pCO_2 under spring temperatures may arise from their need to produce new shell material to replace shell lost to dissolution during the cooler months when external seawater approaches undersaturation with respect to the calcite mineral of scallop shells. Likewise, the apparent diversion of energy toward tissue production with increasing pCO_2 under their summer temperature may reflect their need to accumulate lipid reserves, polysaccharides, and other tissue in support of reproduction in the warmer months—which is also when bivalve shells are less vulnerable to dissolution because of the higher calcite saturation state of their surrounding seawater.

Role of EPF Carbonate Chemistry in King Scallop Calcification Response to Ocean Acidification

Most prior studies exploring links between calcification site pH and calcification response to ocean acidification have investigated scleractinian corals (e.g., Ries 2011a, McCulloch et al. 2012a, Holcomb et al. 2014), with few studies to date focusing on bivalves (Ramesh et al. 2017). In the present study, king scallop EPF pH declined significantly with increasing pCO_2 at 9°C but was uncorrelated with pCO_2 at 12°C (Fig. 3B). Notably, king scallop calcification rate increased with decreasing EPF pH at 9°C and exhibited no change with decreasing EPF pH at 12°C. Ries (2011a) previously published a generalized model of calcifying fluid chemistry showing that a CO_2-induced decline in calcification site pH and concomitant increase in calcification site DIC should reduce calcium carbonate saturation state at the site of calcification (and thus calcification rate) for calcifiers that remove a small number of protons from their calcification site (i.e., "weak proton pumpers"), but should increase saturation state for calcifiers that remove a large number of protons from their calcification site (i.e., "strong proton pumpers") (see also McCulloch et al. 2012a, Holcomb et al. 2014, Sutton et al. 2018). Although the observed decline in king scallop EPF pH with decreasing

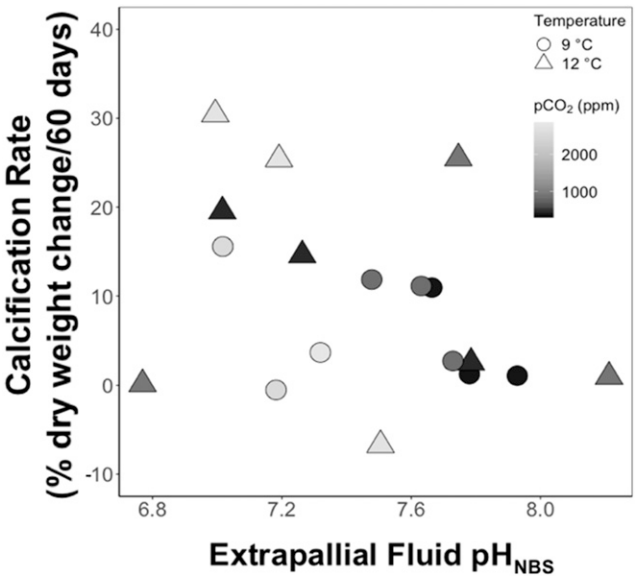

Figure 4. Relationship between king scallop EPF pH_{NBS} and net calcification rate for 12°C (triangles) and 9°C (circles) treatments, across all pCO_2 conditions (grayscale intensity proportional to pCO_2). Calcification rate was inversely correlated with EPF pH at 9°C (LM, $P = 0.033$) when controlling for the effects of pCO_2 on calcification rate (LM, $P = 0.052$) and not significantly correlated with EPF pH at 12°C (LM, $P = 0.397$) when controlling for the effects of pCO_2 on calcification rate (LM, $P = 0.187$).

seawater pH is consistent with this model, the observed resilience of king scallops to ocean acidification (increasing calcification rate with increasing pCO_2 at 9°C; no change at 12°C) is not consistent with the predictions of the model—assuming that the low EPF pH observed in king scallops (i.e., below seawater pH; Fig. 3B) indicates they are "weak proton pumpers." Crenshaw (1972) showed that DIC of the EPF within three species of bivalves was approximately double that of seawater, which raises the possibility that scallops may actually be strong proton pumpers to the extent that they substantially elevate EPF pH relative to EPF pH that is in equilibrium with such highly elevated DIC. If king scallops are indeed strong proton pumpers, then their positive correlation between pCO_2 and calcification rate at 9°C, and lack of correlation at 12°C—both indicating relative resilience to ocean acidification—would be consistent with the predictions of the proton pumping model of ocean acidification response (Ries 2011a). Future studies should aim to measure both DIC and pH of the scallop EPF under a range of pCO_2 and temperature scenarios to further explore this hypothesis.

It should be noted that the positive correlation between pCO_2 and calcification rate, and the inverse correlation between pCO_2 and EPF pH at 9°C, may drive much of the apparent inverse correlation between EPF pH and calcification rate (Fig. 4). Yet, even after controlling for the relationship between pCO_2 and calcification rate at 9°C via the GLM (Table 2), there still exists a significant inverse correlation between EPF pH and calcification rate. Thus, even among replicate specimens within pCO_2 treatments at 9°C, calcification rate was inversely correlated with EPF pH. This observation provides further support for the assertion that some other component(s) of the EPF carbonate system beyond pH—such as DIC (Crenshaw 1972)—must be modified relative to seawater conditions to elevate $CaCO_3$ saturation state of the EPF in support of shell mineralization. Interspecimen differences in EPF DIC, e.g., could arise from differential rates of respiration, which translate into differential rates of calcification as the scallop elevates EPF pH relative to equilibrium pH conditions associated with increased EPF DIC—thereby driving the inverse correlation between EPF pH and calcification rate within pCO_2 treatments in a manner similar to that discussed previously for CO_2-induced increases in EPF DIC across pCO_2 treatments.

Extrapallial fluid pH of adult bivalves is lower than seawater pH under present-day pCO_2 conditions for all bivalve species whose EPF pH has been measured directly (Crenshaw 1972) or inferred from the boron isotopic compositions of the shells of bivalves (a proxy of EPF pH; Sutton et al. 2018). By contrast, Ramesh et al. (2017) found that the pH of the calcification site larvae of the blue mussel *Mytilus edulis* was higher than that of seawater. Shell formed during the larval stage serves a protective function and also acts as ballast and attachment cement during larval settlement, rendering it particularly critical for larval survival and recruitment. Furthermore, larval bivalves are known to produce their shells exclusively from the more soluble aragonite polymorph of $CaCO_3$, whereas adult bivalves produce them from the less soluble calcite polymorph (as is the case with scallops), from the aragonite polymorph, or from a complex multilayered structure of both the calcite and aragonite polymorphs (Lowenstam & Weiner 1989, Marin et al. 2012, Gazeau et al. 2013). It, therefore, makes sense that bivalve larvae, which produce a more soluble polymorph of $CaCO_3$ and use it not only for protection from predators but also for ballast and attachment during settlement, would direct a greater proportion of their energy toward elevating pH at their site of calcification than their adult counterparts that often produce a less soluble polymorph of calcium carbonate and use their shell primarily for protection from predators (although adult oyster shell is also used for substrate attachment). Ramesh et al. (2017) also found that ocean acidification reduced calcification site pH of larval blue mussels, which is consistent with the results of the present study on adult king scallops.

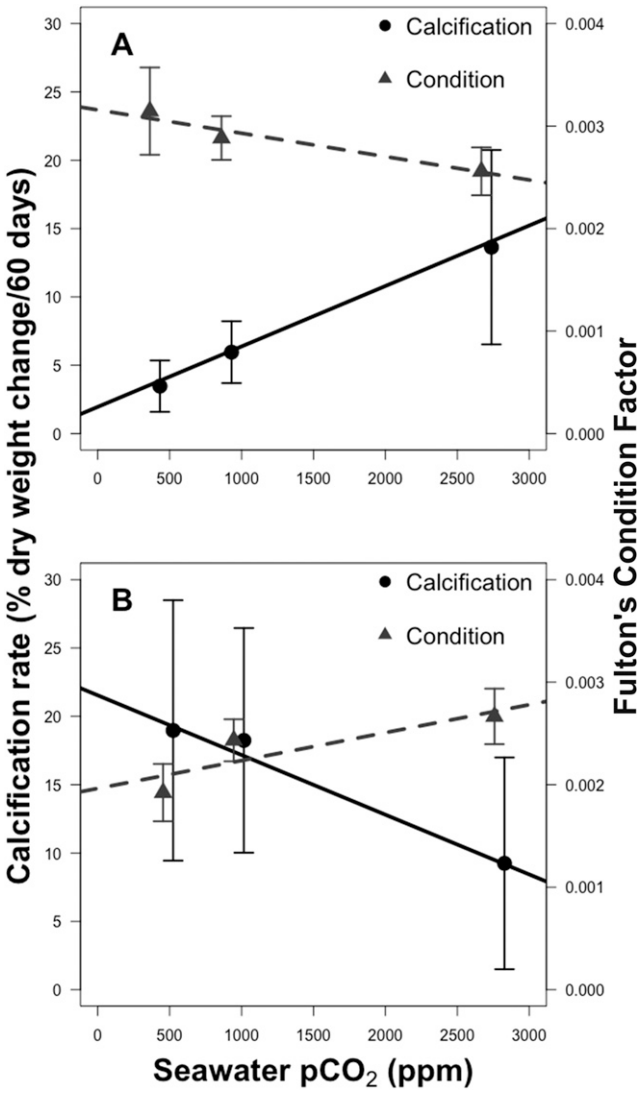

Figure 5. Scatterplot showing reversal of calcification rate and condition factor responses to increasing pCO_2 between spring (9°C) and summer (12°C) temperatures. Data markers corresponding to equivalent pCO_2 treatments have been slightly offset to improve visibility. Vertical bars denote SE.

Although no visible signs of stress (e.g., shell closure, mortality, and reduced feeding) were observed in scallops after implantation of the ports or insertion of the microelectrodes, these are invasive procedures and may have elicited undetected stress responses in the scallops that impacted their ability to regulate EPF pH. The impact of these procedures on the

scallops should have been equivalent under all treatment conditions, so should not be responsible for the different trends observed between EPF pH and pCO_2 at the two temperatures. Nevertheless, future studies aimed at quantifying EPF chemistry of bivalves should assess the impact of these procedures on the physiological status of the study organisms by obtaining physiological measurements, such as respiration rate, before and after port implantation and microelectrode insertion.

CONCLUSIONS

The following conclusions can be drawn from the present study.

(1) The calcification rate of king scallops increased with pCO_2 at 9°C and was invariant with pCO_2 at 12°C, whereas condition factor was invariant with pCO_2 at 9°C and increased with pCO_2 at 12°C. Although these results collectively suggest that king scallops are relatively resilient to ocean acidification, their degree of resilience varied with temperature—highlighting the more general need to assess seasonal differences in the response of marine calcifiers to CO_2-induced ocean acidification.

(2) The trends between condition factor and pCO_2 under the two temperature conditions were exactly opposite to those observed between calcification rate and pCO_2 under the two temperatures, suggesting that king scallops exposed to ocean acidification divert excess energy toward tissue production under summer temperatures (12°C) and toward shell production under spring temperatures (9°C)—potentially reflecting seasonal differences in their physiological demands. Further investigation is needed to determine whether this apparent temperature-dependent diversion of energy between shell and tissue production in response to CO_2-induced ocean acidification is exhibited by other bivalve species.

(3) King scallop EPF pH declined significantly with increasing pCO_2. An inverse correlation existed between scallop EPF pH and calcification rate at 9°C (across and within pCO_2 treatments), but not at 12°C, indicating that EPF pH alone is not controlling the calcification response of king scallops to CO_2-induced acidification. Extrapallial fluid DIC is an important parameter to consider in future studies on this subject.

ACKNOWLEDGMENTS

We thank Gertraud Schmidt (Alfred Wegener Institute), Artur Fink (MPIMM), Laurie Hoffman (MPIMM), Anja Niclas (MPIMM), and Dirk de Beer (MPIMM) for assistance with construction and use of pH microelectrodes; Silvia Hardenberg, Nico Steinel, and Christian Brandt (ZMT) for assistance with animal husbandry and redesign of the acidification system at the ZMT; Matthias Birkicht (ZMT) for assistance with water chemistry analysis; Guy Grieve (Ethical Shellfish Company) for collecting the king scallops; and John Gunnell (Northeastern University) for advice on statistical analysis. This study was funded by the ZMT, NOAA award #NA14NMF4540072 to JBR and JHG, NOAA/MIT SeaGrant awards #NA14OAR41705710004054 and NA18OAR4170105 to JBR, NSF-BIO-OCE award #1437371 to JBR, and a Hanse-Wissenschaftskolleg Fellowship to JBR.

LITERATURE CITED

Addadi, L., D. Joester, F. Nudelman & S. Weiner. 2006. Mollusk shell formation: a source of new concepts for understanding biomineralization processes. *Chem. Eur. J.* 12:980–987.

Al-Horani, F. A., S. M. Al-Moghrabi & D. de Beer. 2003. Microsensor study of photosynthesis and calcification in the scleractinian coral, *Galaxea fascicularis*: active internal carbon cycle. *J. Exp. Mar. Biol. Ecol.* 288:1–15.

Amaral, V., H. N. Cabral & M. J. Bishop. 2012. Moderate acidification affects growth but not survival of 6-month-old oysters. *Aquat. Ecol.* 46:119–127.

Andersen, S., E. S. Grefsrud & T. Harboe. 2013. Effect of increased pCO_2 level on early shell development in great scallop (*Pecten maximus* Lamarck) larvae. *Biogeosciences* 10:6161–6184.

Andersson, A. J. & D. Gledhill. 2013. Ocean acidification and coral reefs: effects on breakdown, dissolution, and net ecosystem calcification. *Annu. Rev. Mar. Sci.* 5:321–348.

Andersson, A. J., F. T. Mackenzie & N. R. Bates. 2008. Life on the margin: implications of ocean acidification on Mg-calcite, high latitude and cold-water marine calcifiers. *Mar. Ecol. Prog. Ser.* 373:265–273.

Barton, A., B. Hales, G. G. Waldbusser, C. Langdon & R. A. Feely. 2012. The Pacific oyster, *Crassostrea gigas,* shows negative correlation to naturally elevated carbon dioxide levels: Implications for near-term ocean acidification effects. *Limnol. Oceanogr.* 57:698–710.

Beniash, E., A. Ivanina, N. S. Lieb, I. Kurochkin & I. M. Sokolava. 2010. Elevated level of carbon dioxide affects metabolism and shell formation in oysters *Crassostrea virginica*. *Mar. Ecol. Prog. Ser.* 419:95–108.

Beukema, J. J. & R. Dekker. 2005. Decline of recruitment success in cockles and other bivalves in the Wadden Sea: possible role of climate change, predation on postlarvae and fisheries. *Mar. Ecol. Prog. Ser.* 287:149–167.

Beukema, J. J., R. Dekker & J. M. Jansen. 2009. Some like it cold: populations of the tellinid bivalve *Macoma balthica* (L.) suffer in various ways from a warming climate. *Mar. Ecol. Prog. Ser.* 384:135–145.

Brennand, H. S., N. Soars, S. A. Dworjanyn, A. R. Davis & M. Byrne. 2010. Impact of ocean warming and ocean acidification on larval development and calcification in the sea urchin *Tripneustes gratilla*. *PLoS One* 5:1–7.

Brierley, A. S. & M. J. Kingsford. 2009. Impacts of climate change on marine organisms and ecosystems. *Curr. Biol.* 19:602–614.

Cabral-Tena, R. A., H. Reyes-Bonilla, S. Lluch-Cota, D. A. Pax-García, L. E. Calderón-Aguilera, O. Norzagaray-López & E. F. Balart. 2013. Different calcification rates in males and females of the coral *Porites panamensis* in the Gulf of California. *Mar. Ecol. Prog. Ser.* 476:1–8.

Cai, W., Y. Ma, B. M. Hopkinson, A. G. Grottoli, M. E. Warner, Q. Ding, X. Hu, X. Yuan, V. Schoepf, H. Xu, C. Han, T. F. Melman, K. D. Hoadley, D. T. Pettay, Y. Matsui, J. H. Baumann, S. Levas, T. Ting & Y. Wang. 2016. Microelectrode characterization of coral daytime interior pH and carbonate chemistry. *Nat. Commun.* 7:11144.

Caldeira, K. & M. E. Wickett. 2003. Anthropogenic carbon and ocean pH. *Nature* 425:365.

Carey, G. 2013. Quantitative methods in neuroscience [online]. Available at: http://psych.colorado.edu/~carey/qmin/QMIN_2013_03_17.pdf.

Cohen, A. L. & T. A. McConnaughey. 2003. Geochemical perspectives on coral mineralization. *Rev. Mineral. Geochem.* 54:151–187.

Crenshaw, M. A. 1972. The inorganic composition of molluscan extrapallial fluid. *Biol. Bull.* 143:506–512.

Curry, G. B. 1982. Ecology and population structure of the recent brachiopod *Terebratulina* from Scotland. *Paleontology*. 25:227–246.

de Beer, D., A. Schramm, C. M. Santegoeds & M. Kühl. 1997. A nitrite microsensor for profiling environmental biofilms. *Appl. Environ. Microbiol.* 63:973–977.

de Jong, E. W., L. Bosch & P. Westbroek. 1976. Isolation and characterization of a Ca^{2+}-binding polysaccharide associated with coccoliths of *Emiliania huxleyi* (Lohmann) Kamptner. *Eur. J. Biochem.* 70:611–621.

Dickinson, G. H., A. V. Ivanina, O. B. Matoo, H. O. Pörtner, G. Lannig, C. Bock, E. Beniash & I. M. Sokolova. 2012. Interactive effects of salinity and elevated CO_2 levels on juvenile eastern oysters, *Crassostrea virginica*. *J. Exp. Biol.* 215: 29-43.

Dixson, D. L., P. L. Munday & G. P. Jones. 2010. Ocean acidification disrupts the innate ability of fish to detect predator olfactory cues. *Ecol. Lett.* 13:68–75.

Dodd, L. F., J. H. Grabowski, M. F. Piehler, I. Westfield & J. B. Ries. 2015. Ocean acidification impairs crab foraging behaviour. *Proc. Biol. Sci.* 282:20150333.

Dupont, S., J. Havenhand, W. Thorndyke, L. Peck & M. Thorndyke. 2008. Near-future level of CO_2-driven ocean acidification radically affects larval survival and development in the brittlestar *Ophiothrix fragilis*. *Mar. Ecol. Prog. Ser.* 373:285–294.

Feely, R. A., S. C. Doney & S. R. Cooley. 2010. Ocean acidification: present conditions and future changes in a high-CO_2 world. *Oceanography* 22:36–47.

Ferrari, M. C. O., M. I. McCormick, P. L. Munday, M. G. Meekan, D. L. Dixson, O. Lonnstedt & D. P. Chivers. 2011. Putting prey and predator into the CO_2 equation—qualitative and quantitative effects of ocean acidification on predator-prey interactions. *Ecol. Lett.* 14:1143–1148.

Fernández-Reiriz, M. J., P. Range, X. A. Álvarez-Salgado& U. Labarta. 2011. Physiological energetics of juvenile clams *Ruditapes decussatus* in a high CO_2 coastal ocean. *Mar. Ecol. Prog. Ser.* 433:97–105.

Frieder, C. A., S. L. Applebaum, T.-C. F. Pan, D. Hedgecock & D. T. Manahan. 2017. Metabolic cost of calcification in bivalve larvae under experimental ocean acidification. *ICES J. Mar. Sci.* 74:941–954.

Gaylord, B., T. M. Hill, E. Sanford, E. A. Lenz, L. A. Jacobs, K. N. Sato, A. D. Russell & A. Hettinger. 2011. Functional impacts of ocean acidification in an ecologically critical foundation species. *J. Exp. Biol.* 214:2586–2594.

Gazeau, F., J.-P. Gattuso, C. Dawber, A. E. Pronker, F. Peene, J. Peene, C. H. R. Heip & J. J. Middelburg. 2010. Effect of ocean acidification on the early life stages of the blue mussel (*Mytilus edulis*). *Biogeosciences* 7:2051–2060.

Gazeau, F., L. M. Parker, S. Comeau, J.-P. Gattuso, W. A. O'Connor, S. Martin, H. O. Pörtner & P. M. Ross. 2013. Impacts of ocean acidification on marine shelled molluscs. *Mar. Biol.* 160:2207–2245.

Gotelli, N. J. & A. M. Ellison. 2013. A primer of ecological statistics, 2nd edition. Oxford, UK: Oxford University Press. pp. 91–106.

Hiebenthal, C., E. E. R. Philipp, A. Eisenhauer & M. Wahl. 2013. Effects of seawater pCO_2 and temperature on shell growth, shell stability, condition and cellular stress of Western Baltic Sea *Mytilus edulis* (L.) and *Arctica islandica* (L.). *Mar. Biol.* 160:2073–2087.

Hilbish, T. J. 1986. Growth trajectories of shell and soft tissue in bivalves: seasonal variation in *Mytilus edulis* L. *J. Exp. Mar. Biol. Ecol.* 96:103–113.

Hohn, S. & A. Merico. 2015. Quantifying the relative importance of transcellular and paracellular ion transports to coral polyp calcification. *Front. Earth Sci.* 2:1–11.

Holcomb, M., A. A. Venn, E. Tambutté, S. Tambutté, D. Allemand, J. Trotter & M. McCulloch. 2014. Coral calcifying fluid pH dictates response to ocean acidification. *Sci. Rep.* 4:5207.

Horvath, K. M., K. D. Castillo, P. Armstrong, I. T. Westfield, T. Courtney & J. B. Ries. 2016. Next-century ocean acidification and warming both reduce calcification rate, but only acidification alters skeletal morphology of reef-building coral *Siderastrea siderea*. *Sci. Rep.* 6:29613.

Iglesias-Rodriguez, A. M. D., P. R. Halloran, R. E. M. Rickaby, I. R. Hall, E. Colmenero-Hidalgo, J. R. Gittins, D. R. H. Green, T. Tyrrell, S. J. Gibbs, P. von Dassow, E. Rehm, E. V. Armbrust & K. P. Boessenkool. 2008. Phytoplankton calcification in a high-CO_2 world. *Science* 320:336–340.

IPCC. 2014. *Climate Change 2014: Synthesis Report*. Contribution of working groups I, II and III to the fifth assessment report of the intergovernmental panel on climate change [Core Writing Team, Pachauri, R. K. & L. A. Meyer, editors.] Geneva, Switzerland: IPCC. 150 pp.

Ivanina, A. V., G. H. Dickinson, O. B. Matoo, R. Bagwe, A. Dickinson, E. Beniash & I. M. Sokolova. 2013. Interactive effects of elevated temperature and CO_2 levels on energy metabolism and biomineralization of marine bivalves *Crassostrea virginica* and *Mercenaria mercenaria*. *Comp. Biochem. Physiol. A Mol. Integr. Physiol.* 166:101–111.

Kroeker, K. J., R. L. Kordas, R. Crim, I. E. Hendriks, L. Ramajo, G. S. Singh, C. M. Duarte & J.-P. Gattuso. 2013. Impacts of ocean acidification on marine organisms: quantifying sensitivities and interaction with warming. *Glob. Change Biol.* 19:1884–1896.

Kroeker, K. J., E. Sanford, B. M. Jellison & B. Gaylord. 2014. Predicting the effects of ocean acidification on predator-prey interactions: a conceptual framework based on coastal molluscs. *Biol. Bull.* 226:211–222.

Lewis, E. & D. W. R. Wallace. 1998. CO2SYS-program developed for CO_2 system calculations [online]. Available at: https://www.nodc.noaa.gov/ocads/oceans/CO2SYS/co2rprt.html.

Lowenstam, H. A. & S. Weiner. 1989. On biomineralization. New York, NY: Oxford University Press. 324 pp.

Lucas, A. & P. G. Beninger. 1985. The use of physiological condition indices in marine bivalve aquaculture. *Aquaculture* 44:187–200.

Mackenzie, C. L., G. A. Ormondroyd, S. F. Curling, R. J. Ball, N. M. Whiteley & S. K. Malham. 2014. Ocean warming, more than acidification, reduces shell strength in a commercial shellfish species during food limitation. *PLoS One* 9:1–9.

Marin, F., N. Le Roy & B. Marie. 2012. The formation and mineralization of mollusk shell. *Front. Biosci.* S4:1099–11251.

McCulloch, M. T., J. P. D'Olivo, J. Falter, M. Holcomb & J. A. Trotter. 2017. Interactive dynamics of pH and DIC upregulation. *Nat. Commun.* 8:15686.

McCulloch, M., J. Falter, J. Trotter & P. Montagna. 2012a. Coral resilience to ocean acidification and global warming through pH upregulation. *Nat. Clim. Chang.* 2:623–627.

McCulloch, M., J. Trotter, P. Montagna, J. Falter, R. Dunbar, A. Freiwald, G. Försterra, M. López Correa, C. Maier, A. Rüggeberg & M. Taviani. 2012b. Resilience of cold-water scleractinian corals to ocean acidification: boron isotopic systematics of pH and saturation state. *Geochim. Cosmochim. Acta* 87:21–34.

Melzner, F., P. Stange, K. Trübenbach, J. Thomsen, I. Casties, U. Panknin, S. N. Gorb & M. A. Gutowska. 2011. Food supply and seawater pCO_2 impact calcification and internal shell dissolution in the blue mussel *Mytilus edulis*. *PLoS One* 6:1–9.

Michaelidis, B., C. Ouzounis, A. Paleras & H. O. Pörtner. 2005. Effects of long-term moderate hypercapnia on acid—base balance and growth rate in marine mussels *Mytilus galloprovincialis*. *Mar. Ecol. Prog. Ser.* 293:109–118.

Mucci, A. 1983. The solubility of calcite and aragonite in seawater at various salinities, temperatures, and one atmosphere total pressure. *Am. J. Sci*. 283:780–799.

Orr, J. C., V. J. Fabry, O. Aumont, L. Bopp, S. C. Doney, R. A. Feely, A. Gnanadesikan, N. Gruber, A. Ishida, F. Joos, R. M. Key, K. Lindsay, E. Maier-Reimer, R. Matear, P. Monfray, A. Mouchet, R. G. Najjar, G.-K. Plattner, K. B. Rodgers, C. L. Sabine, J. L. Sarmiento, R. Schlitzer, R. D. Slater, I. J. Totterdell, M.-F. Weirig, Y. Yamanaka& A. Yool. 2005. Anthropogenic ocean acidification over the twenty-first century and its impact on calcifying organisms. *Nature* 437:681–686.

Parker, L. M., P. M. Ross & W. A. O'Connor. 2010. Comparing the effect of elevated pCO_2 and temperature on the fertilization and early development of two species of oysters. *Mar. Biol*. 157:2435–2452.

Pörtner, H. O. 2002. Climate variations and the physiological basis of temperature dependent biogeography: systemic to molecular hierarchy of thermal tolerance in animals. *Comp. Biochem. Physiol. A Mol. Integr. Physiol*. 132:739–761.

Pörtner, H. O. 2008. Ecosystem effects of ocean acidification in times of ocean warming: a physiologist's view. *Mar. Ecol. Prog. Ser*. 373:203–217.

Pörtner, H. O. & A. P. Farrell. 2008. Physiology and climate change. *Science* 39:398–405.

Pörtner, H. O., A. Reipschlager & N. Heisler. 1998. Acid-base regulation, metabolism and energetics in *Sipunculus nudus* as a function of ambient carbon dioxide level. *J. Exp. Biol*. 201:43–55.

Ramesh, K., M. Y. Hu, J. Thomsen, M. Bleich & F. Melzner. 2017. Mussel larvae modify calcifying fluid carbonate chemistry to promote calcification. *Nat. Commun*. 8:1–8.

Reymond, C. E., A. Lloyd, D. I. Kline, S. G. Dove & J. M. Pandolfi. 2013. Decline in growth of foraminifer *Marginopora rossi* under eutrophication and ocean acidification scenarios. *Glob. Change Biol*. 19:291–302.

Ries, J. B. 2011a. A physicochemical framework for interpreting the biological calcification response to CO_2-induced ocean acidification. *Geochim. Cosmochim. Acta* 75:4053–4064.

Ries, J. B. 2011b. Skeletal mineralogy in a high-CO_2 world. *J. Exp. Mar. Biol. Ecol*. 403:54–64.

Ries, J. B., A. L. Cohen & D. C. McCorkle. 2009. Marine calcifiers exhibit mixed responses to CO_2-induced ocean acidification. *Geology* 37:1131–1134.

Ries, J. B., M. N. Ghazaleh, B. Connolly, I. Westfield & K. D. Castillo. 2016. Impacts of seawater saturation state (Ω_A = 0.4–4.6) and temperature (10, 25 °C) on the dissolution kinetics of whole-shell biogenic carbonates. *Geochim. Cosmochim. Acta* 192:318–337.

Roy, R. N., L. N. Roy, K. M. Vogel, C. Porter-Moore, T. Pearson, C. E. Good, F. J. Millero & D. M. Campbell. 1993. The dissociation constants of carbonic acid in seawater at salinities 5 to 45 and temperatures 0 to 45 °C. *Mar. Chem*. 44:249–267.

Sanders, M. B., T. P. Bean, T. H. Hutchinson & W. J. F. Le Quesne. 2013. Juvenile king scallop, *Pecten maximus*, is potentially tolerant to low levels of ocean acidification when food is unrestricted. *PLoS One* 8:1–13.

Schalkhausser, B., C. Bock, K. Stemmer, T. Brey, H. O. Pörtner & G. Lannig. 2013. Impact of ocean acidification on escape performance of the king scallop, *Pecten maximus*, from Norway. *Mar. Biol*. 160:1995–2006.

Sutton, J. N., Y.-W. Liu, J. B. Ries, M. Guillermic, E. Ponzevera & R. A. Eagle. 2018. $\delta^{11}B$ as monitor of calcification site pH in divergent marine calcifying organisms. *Biogeosciences* 15:1447–1467.

Talmage, S. C. & C. J. Gobler. 2009. The effects of elevated carbon dioxide concentrations on the metamorphosis, size, and survival of larval hard clams (*Mercenaria mercenaria*), bay scallops (*Argopecten irradians*), and Eastern oysters (*Crassostrea virginica*). *Limnol. Oceanogr*. 54:2072–2080.

Talmage, S. C. & C. J. Gobler. 2011. Effects of elevated temperature and carbon dioxide on the growth and survival of larvae and juveniles of three species of northwest Atlantic bivalves. *PLoS One* 6:1–12.

Thomsen, J. & F. Melzner. 2010. Moderate seawater acidification does not elicit long-term metabolic depression in the blue mussel *Mytilus edulis*. *Mar. Biol*. 157:2667–2676.

Trotter, J., P. Montagna, M. McCulloch, S. Silenzi, S. Reynaud, G. Mortimer, S. Martin, C. Ferrier-Pagès, J.-P. Gattuso & R. Rodolfo-Metalpa. 2011. Quantifying the pH 'vital effect' in the temperate zooxanthellate coral *Cladocora caespitosa*: validation of the boron seawater pH proxy. *Earth Planet. Sci. Lett*. 303:163–173.

Venn, A., É. Tambutté, M. Holcomb, D. Allemand & S. Tambutté. 2011. Live tissue imaging shows reef corals elevate pH under their calcifying tissue relative to seawater. *PLoS One* 6:1–9.

Waldbusser, G. G., E. L. Brunner, B. A. Haley, B. Hales, C. J. Langdon & F. G. Prahl. 2013. A developmental and energetic basis linking larval oyster shell formation to acidification sensitivity. *Geophys. Res. Lett*. 40:2171–2176.

Waldbusser, G. G., B. Hales, C. J. Langdon, B. A. Haley, P. Schrader, E. L. Brunner, M. W. Gray, C. A. Miller & I. Gimenez. 2014. Saturation-state sensitivity of marine bivalve larvae to ocean acidification. *Nat. Clim. Chang*. 5:273–280.

Waldbusser, G. G., B. Hales, C. J. Langdon, B. A. Haley, P. Schraeder, E. L. Brunner, M. W. Gray, C. A. Miller, I. Gimenez & G. Hutchinson. 2015. Ocean acidification has multiple modes of action on bivalve larvae. *PLoS One* 10:1–29.

Waldbusser, G. G., E. P. Voigt, H. Bergschneider, M. A. Green & R. I. E. Newell. 2011. Biocalcification in the Eastern Oyster (*Crassostrea virginica*) in relation to long-term trends in Chesapeake Bay pH. *Estuaries Coasts* 34:221–231.

Wall, M., F. Ragazzola, L. C. Foster, A. Form & D. N. Schmidt. 2015. pH up-regulation as a potential mechanism for the cold-water coral *Lophelia pertusa* to sustain growth in aragonite undersaturated conditions. *Biogeosciences* 12:6869–6880.

Watson, S.-A., P. C. Southgate, P. A. Tyler & L. S. Peck. 2009. Early larval development of the Sydney rock oyster *Saccostrea glomerata* under near-future predictions of CO_2-driven ocean acidification. *J. Shellfish Res*. 28:431–437.

Weiner, S. & W. Traub. 1984. Macromolecules in mollusc shells and their functions in biomineralization. *Philos. Trans. R. Soc. Lond. B Biol. Sci*. 304:425–434.

Welladsen, H. M., P. C. Southgate & K. Heimann. 2010. The effects of exposure to near-future levels of ocean acidification on shell characteristics of *Pinctada fucata* (Bivalvia: Pteriidae). *Molluscan Res*. 30:125–130.

Wheeler, A. P. & C. S. Sikes. 1984. Regulation of carbonate calcification by organic matrix. *Am. Zool*. 24:933–944.

White, M. M., D. C. McCorkle, L. S. Millineaux & A. L. Cohen. 2013. Early exposure of bay scallops (*Argopecten irradians*) to high CO_2 causes a decrease in larval shell growth. *PLoS One* 8:e61065.

Wilbur, K. M. & A. M. Bernhardt. 1984. Effects of amino acids, magnesium, and molluscan extrapallial fluid on crystallization of calcium carbonate: in vitro experiments. *Biol. Bull*. 166:251–259.

Zhuravlev, A. Y. & R. A. Wood. 2009. Controls on carbonate skeletal mineralogy: global CO_2 evolution and mass extinctions. *Geology* 37:1123–1126.

TABLE A1.

Evaluation of calcification rate model via AIC, with chosen models shown in bold.

Calcification rate model selection					
Model	**Temperature**	**AIC**	**Response variable**	***t*-value**	***P*-value**
$pCO_2 \times$ temperature	Both	251.770	pCO_2	1.619	0.117
			Temperature	2.181	0.038**
			$pCO_2 \times$ temperature	–1.634	0.114
pCO_2	**9°C**	**114.010**	**pCO_2**	**1.787**	**0.097***
pCO_2	**12°C**	**133.710**	**pCO_2**	**–0.914**	**0.377**
Temperature	Both	250.710	Temperature	1.443	0.160

* Significance at $\alpha = 0.10$.
** Significance at $\alpha = 0.05$.

TABLE A2.

Evaluation of EPF pH model via AIC, with chosen models shown in bold.

EPF pH model selection					
Model	**Temperature**	**AIC**	**Predictor variable**	***t*-value**	***P*-value**
$pCO_2 \times$ temperature	Both	19.342	pCO_2	–1.249	0.232
			Temperature	–1.212	0.246
			$pCO_2 \times$ temperature	0.967	0.350
pCO_2 + temperature	Both	18.506	pCO_2	–2.071	0.056*
			Temperature	–0.731	0.476
pCO_2	**Both**	**17.136**	**pCO_2**	**–2.139**	**0.048****
pCO_2	**9°C**	**–5.883**	**pCO_2**	**–5.368**	**<0.001*****
pCO_2	**12°C**	**16.160**	**pCO_2**	**–0.584**	**0.577**

* Significance at $\alpha = 0.10$.
** Significance at $\alpha = 0.05$.
*** Significance at $\alpha = 0.001$.

TABLE A3.

Evaluation of calcification rate model (including EPF pH as predictor) via AIC, with chosen model shown in bold.

Calcification rate model selection: models with EPF pH					
Model	**Temperature**	**AIC**	**Response variable**	***t*-value**	***P*-value**
pCO_2 × temperature × EPF pH	Both	141.470	pCO_2	–0.257	0.802
			Temperature	–1.388	0.195
			EPF pH	–1.012	0.335
			pCO_2 × temperature	1.314	0.218
			pCO_2 × EPF pH	0.204	0.842
			Temperature × EPF pH	1.407	0.190
			Temperature × pCO_2 × EPF pH	–1.275	0.231
pCO_2 × EPF pH	9°C	76.838	pCO_2	1.526	0.187
			EPF pH	0.926	0.397
			pCO_2 × EPF pH	–1.514	0.190
pCO_2 + EPF pH	**9°C**	**57.111**	**pCO_2**	**–2.424**	**0.052***
			EPF pH	**–2.754**	**0.033****
EPF pH	9°C	61.256	EPF pH	–1.007	0.348
pCO_2	9°C	114.010	pCO_2	1.787	0.097*
pCO_2 × EPF pH	**12°C**	**20.388**	**pCO_2**	**1.526**	**0.187**
			EPF pH	**0.926**	**0.397**
			pCO_2 × EPF pH	**–1.514**	**0.190**
pCO_2 + EPF pH	12°C	78.235	pCO_2	0.350	0.738
			EPF pH	–0.733	0.491
EPF pH	12°C	76.417	EPF pH	–0.885	0.406
pCO_2	12°C	133.710	pCO_2	–0.914	0.377

* Significance at $\alpha = 0.10$.
** Significance at $\alpha = 0.05$.

TABLE A4.

Evaluation of condition factor model via AIC, with chosen model shown in bold.

Condition factor model selection					
Model	**Temperature**	**AIC**	**Predictor variable**	***t*-value**	***P*-value**
pCO_2 × temperature	**Both**	**–352.450**	**pCO_2**	**-2.146**	**0.041****
			Temperature	**–3.143**	**0.004*****
			pCO_2 × temperature	**2.196**	**0.037****
pCO_2	9°C	–173.120	pCO_2	–1.320	0.210
pCO_2	12°C	–177.670	pCO_2	1.833	0.089*
Temperature	Both	–351.31	Temperature	–2.201	0.036**

* Significance at $\alpha = 0.10$.
** Significance at $\alpha = 0.05$.
*** Significance at $\alpha = 0.01$.